EVALUATION OF THE ZIGBEE TRANSMISSION REPETITION MECHANISM IN THE VARIABLY-LOADED REVERBERATION CHAMBER

K. Staniec[*]

Institute of Telecommunications, Teleinformatics and Acoustics, Wroclaw University of Technology, Wroclaw, Poland

Abstract—The purpose of this paper is to provide both qualitative and quantitative assessment of one of the methods for providing reliable transmission in the ZigBee system. After intensive research on the time delay spread in a variably loaded reverberation chamber, this facility was then used to measure the Packet Error Rate under multipath conditions ranging from an unloaded to an overloaded chamber case. In all measurements, the key parameter was the number of allowed packet repetitions (retries). Eventually, recommendations were given regarding the optimal use of retries and their impact on ZigBee performance under different multipath scenarios obtained in the reverberation chamber and related to particular propagation environments to which these conditions are typical.

1. INTRODUCTION

The recent decade has been marked by a rapid growth of interest in applications involving the deployment of wireless sensor networks (some examples given in [1–3]). It has been in fact envisaged in Reference [4] at the end of the former century as one of the 21 key ideas that would drive the technical progress in the 21st century. Unfortunately, as has already occurred multiple times, the technical development is not always followed by its users' awareness of some possible weaknesses and threats that need to be considered in order to efficiently use a particular system. One such threat is the multipath effect present — to a different degree — in all propagation environments and which affects digital systems differently depending on transmission techniques implemented in them. In this article

attention will be put on one of the most widespread and popular systems for transmitting low-data rate sensor data over radio. ZigBee uses the direct sequence spread spectrum (DSSS) transmission and as such is rather susceptible to negative multipath effects. For this reason, a reverberation chamber has been accustomed to emulate various propagation environments, by adjusting the time delay spread with a controlled number of absorbing panels. Since the ZigBee (or rather IEEE 802.15.4) specification allows the use of multiple repetitions (retries) of the same message in case of reception failure, the effectiveness of this methods has been tested providing both quantitative and qualitative results along with recommendations for a smart application of this technique in order to avoid some consequences impairing the system performance if the retries are set to excessive values.

2. ON THE RADIO CHANNEL TIME PROPERTIES

The analysis of the radio channels as a time-dispersive medium shall start with the observation that the emitted signal will propagate by interacting with the surrounding environment, that involves reflections from objects, transmissions thru obstacles, diffraction on edges and scattering from rough surface. Thus, the signal arriving at the receiver will not come in a single fringe, but as a pack of signals with different amplitudes, phases, angles of arrival, and short time delays, being delayed copies of the original signal ([5, 6, 9]). Once collected within a certain time span at a receiver, they sum up in a vector fashion, accounting for their relative phase differences, which causes some copies to overlap constructively if both are in phase or cancel out otherwise. Such behavior leads to *small-scale fading*, which is a typical propagation effect, especially in the indoor and urban environment. Since the received signal in a multipath channel consists of a series of attenuated, time-delayed, phase-shifted replicas of the transmitted signal, the baseband impulse response of a multipath channel can be given by Equation (1). Hence, the radio channel can be mathematically represented at any point in a three-dimensional space as a linear, time-
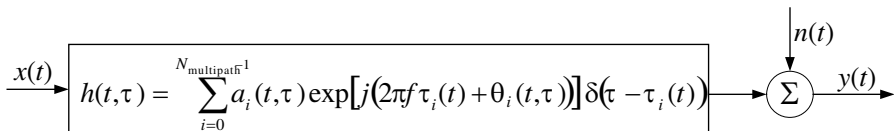

$$x(t) \quad h(t,\tau) = \sum_{i=0}^{N_{\text{multipath}}-1} a_i(t,\tau) \exp\left[j\left(2\pi f\tau_i(t) + \theta_i(t,\tau)\right)\right]\delta\left(\tau - \tau_i(t)\right) \quad \xrightarrow{n(t)} \Sigma \quad y(t)$$

Figure 1. The wideband radio channel model.

variant filter (Fig. 1). The time variance appears here due to the temporal changes in real propagation environments, such as the motion of people, replacement of objects etc.

$$h(t, \tau) = \sum_{i=0}^{N_{\text{multipath}}-1} a_i(t, \tau) \exp\left[j\left(2\pi f \tau_i(t) + \theta_i(t, \tau)\right)\right] \delta\left(\tau - \tau_i(t)\right) \quad (1)$$

$$H(f) = \int_{-\infty}^{\infty} h(t, \tau) e^{-j2\pi ft} dt \quad (2)$$

In Equation (1), $h(t, \tau)$ is the radio channel impulse response, $N_{\text{multipath}}$ is the number of multipath components, $a_i(t, \tau)$ and τ_i are the real amplitudes and excess delays, respectively, of i-th component at time t [9]. The phase term $2\pi f \tau_i(t) + \theta_i(t, \tau)$ represents the phase shift due to free space propagation of the i-th component, plus any additional phase shifts which are encountered in the channel. The frequency response $H(f)$ can be easily obtained from the Fourier transform of $h(t)$ as by Equation (2). Therefore, since either $h(t)$ or $H(f)$ are needed for an exhaustive characterization of the radio channel, only one of these should be measured (or accurately predicted), while the other one will be obtained by means of the Fourier transform or its inverse. Now, assuming that the signal is transmitted into an AWGN (Additive White Gaussian Noise) radio channel, the output signal will be in the form given by Equation (3), where $x(t)$, $n(t)$ and $y(t)$ represent, respectively, the input signal, the channel white noise and the channel output signal.

$$y(t) = \int_{-\infty}^{\infty} x(\tau) h(t, \tau) d\tau + n(t) \quad (3)$$

Crucial parameters with which to identify the characteristics of such a channel are: the mean excess delay, the root-mean square (rms) delay spread τ_{rms}, delay window, total energy, coherence (correlation bandwidth) $B_{x\%}(f)$ and the Power Delay Profile (PDP). The parameters of particular importance to PCS (Personal Communications System) systems design are PDP, τ_{rms}, $B_{x\%}(f)$. PDP represents the time distribution of the received signal power from a transmitted impulse, and is defined by Equation (4). It is often used to quantify time dispersion in mobile channels, and hence it characterizes the channel frequency selectivity. The mean excess delay τ_m is the first moment of the power delay profile and is defined by Equation (5) and has the sense of the first moment of the PDP. Finally, τ_{rms}, having the sense of the second central moment of the PDP, see Equation (6),

is a measure of the channel time dispersiveness and determines the maximum symbol rate achievable by a communication system before inter-symbol interference (ISI) occurs (see also [7, 8] for details).

$$\text{PDP}(t, \tau) = |h(t, \tau)|^2 = \sum_{i=0}^{N_{\text{multipath}}-1} a_i^2 \delta(t - \tau_i(t)) \tag{4}$$

$$\tau_m = \frac{\sum_i a_i^2 \tau_i}{\sum_i a_i^2} = \frac{\sum_i P(\tau_i)\tau_i}{\sum_i P(\tau_i)} \tag{5}$$

$$\tau_{\text{rms}} = \sqrt{\bar{\tau}^2 - (\tau_m)^2} \tag{6}$$

where

$$\bar{\tau}^2 = \frac{\sum_i a_i^2 \tau_i^2}{\sum_i a_i^2} = \frac{\sum_i P(\tau_i)\tau_i^2}{\sum_i P(\tau_i)} \tag{7}$$

In [7], $B_{x\%}(\Delta f_{x\%})$ is defined by Equation (8) as the Fourier transform of PDP, where $\Delta f_{x\%}$ denotes frequency range, for which signal components are correlated at $x\%$, where x is usually found to be 50%, or 70–90% [7, 9, 10].

$$B_{x\%}(\Delta f_{x\%}) = \int_{t_0}^{\tau_{\text{max}}} \text{PDP}(\tau)e^{-j2\pi\Delta f_{x\%}\tau}d\tau \tag{8}$$

It is therefore a statistical measure of a frequency range over which signal spectrum undergo approximately equal attenuation and a linear change in phase [9]. Coherence bandwidth has been related by inverse proportionality to τ_{rms} as in Equation (9), where α is bound by values ranging from 5 to 50 [11–13] (which corresponds to the correlation values of 50% and 90%, respectively) or equals 2π if PDP is exponentially distributed.

$$B_{x\%} = \frac{1}{\alpha_b \tau_{\text{rms}}} \tag{9}$$

In [14, 15] a lower bound on the value of $B_{x\%}$ is found to be (10):

$$B_{x\%} \geq \frac{\arccos(x/100)}{\pi\tau_{\text{rms}}} \tag{10}$$

As reported in multiple literature sources (e.g., [9, 14, 16–18]) where the dispersive parameters of various radio channels were both measured and simulated, the values of τ_{rms} lie between 5 ns and 200 ns in indoor environments. In microcells, τ_{rms} is usually found between

0.35 µs and 2 µs. In macrocells, values around 5 µs and more were measured for rural and hilly terrains (see also Table 2 of Section 4). As a rule of thumb (e.g., in [9, 19]) one may assume that if a digital signal has a symbol duration exceeding ten times the rms delay spread, than an equalizer will not be required to achieve $BER \leq 10^{-3}$. If, however, values of τ_{rms} approach or exceed the tenth of the symbol duration, errors due the frequency selectivity of the channel will occur and channel equalization at the receiver is necessary. Equation (11) relates this rule to the maximum achievable data rate R_b:

$$\max(R_b) = 0.1/\tau_{\mathrm{rms}} \tag{11}$$

3. IEEE 802.15.4 SPECIFICATION (ZIGBEE)

3.1. General Facts on ZigBee

Out of the multiplicity of candidate solutions for effective creation of sensor networks is the ZigBee standard based on IEEE 802.15.4 specification [20]. It defines a low-cost, low-range, power-saving system allowing data rates — depending on the frequency band, of 20, 40 and up to 250 kbits/s and almost inexhaustible number of network nodes (typically 16 bit allocated for addressing with or 64 bits using extended addresses). It has been defined in 3 separate bands with twenty seven 2 MHz-wide distinct channels (see Fig. 2(b)) defined therein, as given in Table 1.

Depending on the application requirements, an IEEE 802.15.4 LR-WPAN (Low-Rate Wireless Personal Area Network) may operate in either of two topologies: the star topology or the peer-to-peer topology. In the star topology communication is established between devices and a single central controller, called the PAN coordinator. The peer-to-peer topology also has a PAN coordinator; however, it differs from the star topology in that any device may communicate with any other device as long as they are in range of one another. Peer-to-peer topology allows more complex network formations to be

Table 1. Radio channels and modulations in ZigBee (according to IEEE 802.15.4 spec.).

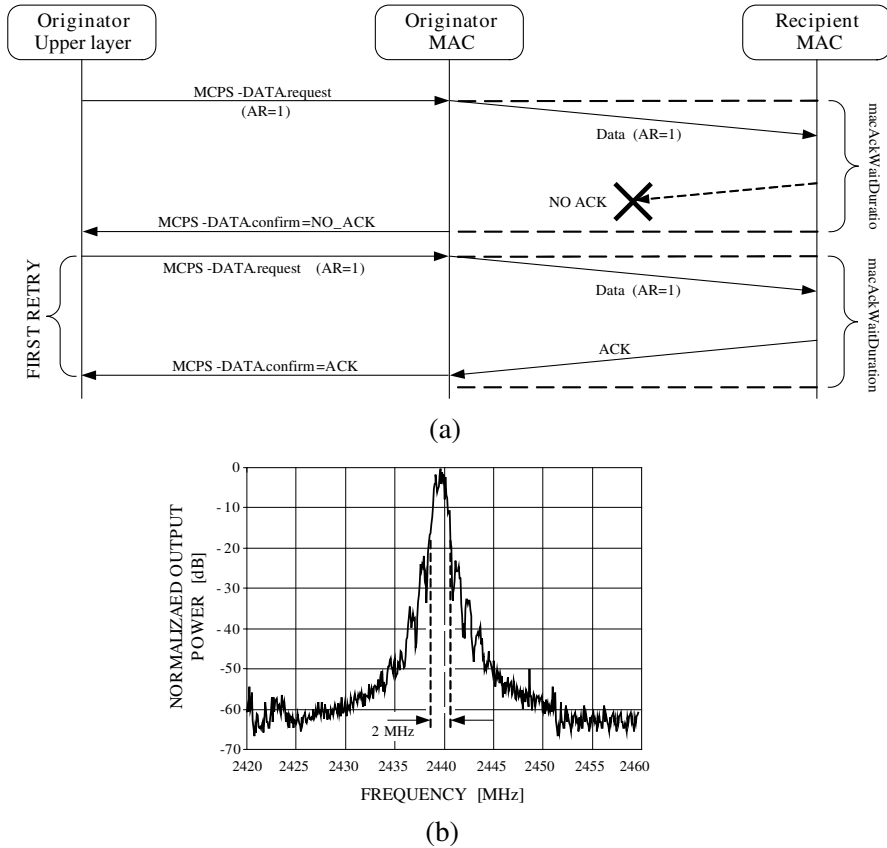| Frequency band	Channels (k)	k-th channel definition	Modulation
868.0–868.6 MHz	$k = 0$	$F_k = 868.3$	BPSK, O-QPSK (DSSS)
902–928 MHz	$k = 1, 2, \ldots, 10$	$F_k = 906 + 2(k-1)$	ASK (Parallel SS)
2400–2483.5 MHz	$k = 11, 12, \ldots, 26$	$F_k = 2405 + 5(k-11)$	O-QPSK (DSSS)

(a)

(b)

Figure 2. (a) Successful data transmission with an acknowledgement and a single retry; (b) measured ZigBee channel spectrum.

implemented, such as mesh networking topology. Applications such as industrial control and monitoring, wireless sensor networks, asset and inventory tracking, intelligent agriculture, and security would benefit from such a network topology. A peer-to-peer network can be ad hoc, self-organizing, and self-healing. It may also allow multiple hops to route messages from any device to any other device on the network although such functionalities are up to higher OSI/ISO layers and are not part of the 802.15.4 specification.

3.2. Repetition Mechanism in ZigBee

The IEEE 802.15.4 LR-WPAN employs various mechanisms to improve the probability of successful data transmission. These mechanisms are:

1. the CSMA-CA mechanism, 2. the data verification and 3. the frame acknowledgment. The first of these consists of two types of channel access schemes, i.e., the non-beacon enabled and the beacon-enabled mode (more on this in chpt. 5.5.4.1 of [20]). The second mechanisms refers to detection of bit errors. A Frame Check Sequence mechanism is employed here using a 16-bit ITU — Telecommunication Standardization Sector (ITU-T) cyclic redundancy check (CRC) for error detection per every frame. Of our interest, however, is the third of these mechanisms. According to [20]: "a successful reception and validation of a data or MAC command frame can be optionally confirmed with an acknowledgment. If the receiving device is unable to handle the received data frame for any reason, the message is not acknowledged. If the originator does not receive an acknowledgment after some period, it assumes that the transmission was unsuccessful and retries the frame transmission. If an acknowledgment is still not received after several retries, the originator can choose either to terminate the transaction or to try again. When the acknowledgment is not required, the originator assumes the transmission was successful". Whether retransmissions are required or not, depends on the current setting of the Acknowledgement Request (AR) subfield of the frame. It is either set to zero (if no retries are requested) or to one (otherwise). The number of retransmissions R is defined by the *macMaxFrameRetries* parameter which may take on values between 0 and 7, three being default [20]. The other parameter important in the retransmission mechanism is the *macACKWaitDuration*, see Equation (12), which defines a period of time for which the message originator awaits the advent of an acknowledgement. The components used in Equation (12) are expressed as multiples of the symbol time duration which may assume values from 16 µs up to 80 µs depending on the physical mode (as in Table 19 of [20]). Since the idea behind this process is rather intuitive it will not be discussed here in depth (for more information refer to chpt. 7.5.6.4 of [20]). In our case, since the 2400–2483.5 MHz O-QPSK mode was used, the symbol duration was 16 µs. A schematic view of transmission with an acknowledgement is shown in Fig. 2. It is a task of upper layer mechanisms to force an acknowledgement mode by setting the Acknowledgement Request (AR) field to one. Then, if the acknowledgement frame is missing (which is indicated by *MCPS-DATA.confirm* primitive set to NO_ACK value) after *macACKWaitDuration* time has elapsed, upper layer entities may ask for packet retransmission up to *macMaxFrameRetries* times.

$$
\begin{aligned}
macACKWaitDuration \; = \; & aUnitBackoffPeriod + aTurnaroundTime \\
& + \lceil 6 * phySymbolsPerOctet \rceil
\end{aligned} \tag{12}
$$

where: $aUnitBackoffPeriod$ = 20, $aTurnaroundTime$ = 12 $phySymbolsPerOctet$ = 0.4, 1.6, 2, 8.

4. THE ITEMS UNDER INVESTIGATION AND A RATIONALE

This article can be viewed as an extension to the research on the ZigBee behavior in low-loss closed structures described in [21] where intensive research was made on the behavior of IEEE 802.15.4 devices in an unloaded reverberation chamber. It is also somewhat similar to [22] where some ZigBee measurements for different chamber loading were also carried out on a single ZigBee channel but with no explicit information on the number of the packet repetition times (retries). As will be presented in further sections, this parameter has a significant effect on the ZigBee performance under heavy-multipath conditions and is usually set to three by default (as advised in IEEE 802.15.4 specification [20] and also implemented in our tested devices). It should therefore be kept in mind that the modulation-coding schemes in the "pure form" can only be studied with the number of retries set to zero. For any other number of retransmissions, what is really being investigated is rather the performance of upper-layer mechanisms for reliable transmission assurance.

In this paper the Packet Error Rate (PER) in ZigBee was tested in three situations:

- for all 16 radio channels available in the 2.4 GHz ISM (Industrial, Scientific and Medical) band (Section 6);
- at a variable chamber load (starting with an unloaded chamber and ending with an overloaded chamber, see Section 7). Since each load scenario generates a particular time delay spread τ_{rms} in the chamber, these values could be associated with different propagation environments (as given in Table 2);

Table 2. Typical RMS delay spreads (according to [18]).

Environment type	RMS delay spread range τ_{rms} [μs]
Indoor cells	0.01–0.05
Mobile satellite	0.04–0.05
Open area	< 0.2
Suburban macrocell	< 1
Urban macrocell	1–3
Hilly area macrocell	3–10

- for different numbers of packet repetitions (beginning with zero, ending with 7 repetitions, see Section 8).

5. MEASUREMENT SET-UP

Measurements were performed in the reverberation chamber located at Wroclaw University of Technology. Its dimensions as well as the placement of the tested ZigBee devices can be seen in Fig. 3. A radio link was set up between two devices located at the height of 54 cm above the chamber ground: one being a simple end-device (or a "slave"), the other being a controller board (or a "master") possessing features allowing to perform PER tests and initiating communication sessions.

The devices used in the experiments were Jennic 5139 equipment, programmed with the use of Jennic JN51xxd Flash Programmer 1.7.2 accordingly to the needs. Each device had a 0 dBi PCB-mounted antenna and they were set to 0 dBm of the output power. Each measured PER value was logged after sending at least 16 thousand packets between the devices in order to acquire statistical robustness and stabilization of results in the highly multipath conditions of the reverberation chamber.

In all measurements it was also assumed that the limiting number of absorbers, for which the reverberation chamber was considered as overloaded, was twelve. This value corresponds to results presented in [25] and denotes the number of absorbing panels for which the delay
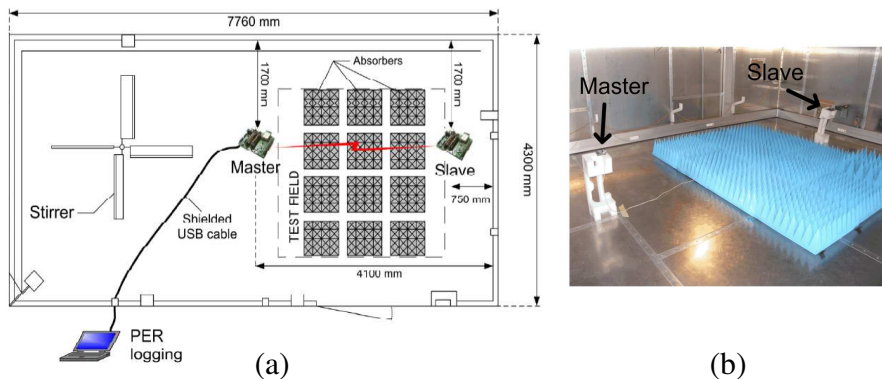

Figure 3. A measurement set-up for PER test of ZigBee devices in the reverberation chamber: (a) a schematic view; (b) a photo of the scene with 12 absorbers.

spread obtained in the chamber reached a stable level (~ 200 ns) and did not noticeably respond to further increase of the load.

6. THE TIME DELAY SPREAD EFFECT ON THE ZIGBEE CHANNEL NUMBER

The first subject of measurements consisted of testing the influence of the radio channel time response existing in the reverberation chamber (under a variable load) on the ZigBee channel number (1 through 16). For this reason, a continuous transmission was established between the master and slave devices while the stirrer was making its full rotation. The procedure was carried out for each of the 16 ZigBee radio channels available in the 2.4 GHz ISM band. After tests were performed in an unloaded reverberation chamber, the same routines were then repeated with a single absorber panel placed inside, then two absorbers and up to twelve, each time increasing the number of panels by two. The devices were operating in an unacknowledged mode, i.e., no confirmations of positive reception were requested on the transmitting side, which was achieved by setting the number of retries to zero in order to prevent upper-layer mechanisms (such as repetitions) from affecting the outcomes.

In these investigations, a Successful Reception Rate (SRR) was used as a measure of ZigBee transmission properties. It is defined simply as a PER's complement to unity and presented as a percentage, i.e., $\mathrm{SRR} = (1 - \mathrm{PER}) * 100\%$. As can be seen in Fig. 4(a), the average SRR quite expectedly rises with the increase of the reverberation
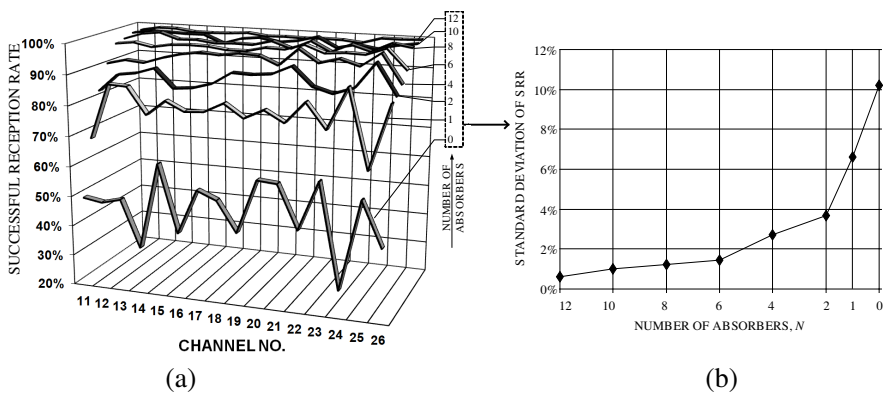

(a) (b)

Figure 4. SRR measurement and its standard deviation at different radio channels and a variably loaded reverberation chamber.

chamber load, reaching almost 100% in the overloaded chamber (i.e., with 12 absorbers). As also turns out, PER variations with the channel number are remarkable when the chamber is lightly loaded, i.e., up to 35% in PER between channels Nos. 15 and 24. As more absorbers are placed, the channel number does not matter that much, yielding merely 2% of maximum variation in the overloaded case. Taking the standard deviation (see the right corner of Fig. 4) as a measure of SRR variation over all 16 channels, one can notice that it is exponentially related to the chamber load. It starts with 0.6% for the least-multipath scenario (12 absorbers) and exceeds 10% in the most reverberant case (i.e., without any absorbers). It is left for further research to examine how the stirrer rotation speed affects this non-uniformity, since it was found in [22] to have some impact on PER (although based on measurements carried out on a single channel).

7. PER AS A FUNCTION OF THE REVERBERATION CHAMBER LOAD

In this part of experiment PER was investigated as a function of the variable reverberation chamber load. These investigations are closely related to previous research, presented in [23–26] where measurements were conducted to obtain the excess delay spread $\tau_{\rm rms}$ for a different number of absorbers.

Since it has been demonstrated that the obtained $\tau_{\rm rms}$ profile vs. load is very dependent on the chamber physical dimensions, no single universal formula can be proposed to relate $\tau_{\rm rms}$ to the number of absorbers N. The common feature of all reverberation chambers, however, is the exponential decay of the excess delay spread with N. In [25], for instance, it was found by Pomianek in measurements and by Staniec in simulations (see also [27] as well as related articles [28–30]), that $\tau_{\rm rms}$ declines with an exponent of -0.69, as shown in Fig. 5(b). The time delay spread, in turn, can be further associated with a particular propagation environment type (see black fields in Fig. 5), according to Table 2 in Section 4. From this association appears that in environments to which ZigBee is best suited (i.e., indoor and open space corresponding to large N), multipath does not pose a great threat since the measured PER is less than 5% in all cases (1% could be reached with a single repetition). The situation becomes less optimistic, however, in suburban (characterized by $\tau_{\rm rms}$ below 1 μs) and urban macrocells (with $\tau_{\rm rms}$ above 1 μs). In those types of environments, the use of more retries may turn out to be necessary to avoid excessive rise of PER. In Fig. 5(a) eight curves have been drawn, each representing PER(N) for a certain number of
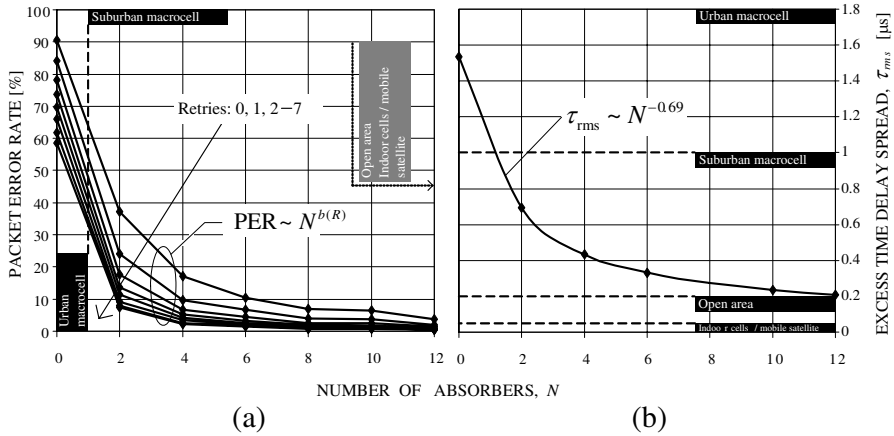
Figure 5. Measurements of: (a) PER and (b) the excess time delay τ_{rms} best-fit curve as a function of the number of absorbers N (the rev. chamber load).

retries R; the upmost curve representing the unacknowledged mode and the bottom one being the scenario allowing up to 7 repetitions R in case of failed packet reception. As can be seen the Packet Error Rate behaves in a similar manner to τ_{rms}, i.e., it exponentially decreases as the chamber is being loaded, at a rate proportional to $N^{b(R)}$. As regards the number of retries R, under highly multipath circumstances PER differs greatly between extremes numbers of R. For instance, in the worst-case scenario of the unloaded reverberation chamber PER reached 90.5% for zero and 58.6% for 7 retries, making almost 32% difference.

In the next step, quantitative evaluation of the $b(R)$ exponent was examined. For this reason, best-fit parameters were determined for each of the eight curves PER $\sim N^b$ in order to check whether any regularity exists between the rate of PER decline with N. It turns out that the increasing number of repetitions causes a linear increase in the $b(R)$ exponent in accordance with Equation (13) being a best-fit to values obtained in measurements (see Table 3). In other words, as more retries are permitted, the more resilient ZigBee system becomes to the multipath radio channel in both quantitative and qualitative manner. The former (i.e., the quantitative manner) is rather clear from Fig. 5 in that PER curves representing greater R tend to lie lower on the PER(N) plot. The latter (i.e., the qualitative manner) is expressed in the faster rate of descent of PER curves with increasing N. Put differently: the greater the number of allowed repetitions,

Table 3. Variation of the exponent '$b(R)$' in PER(N) dependency.

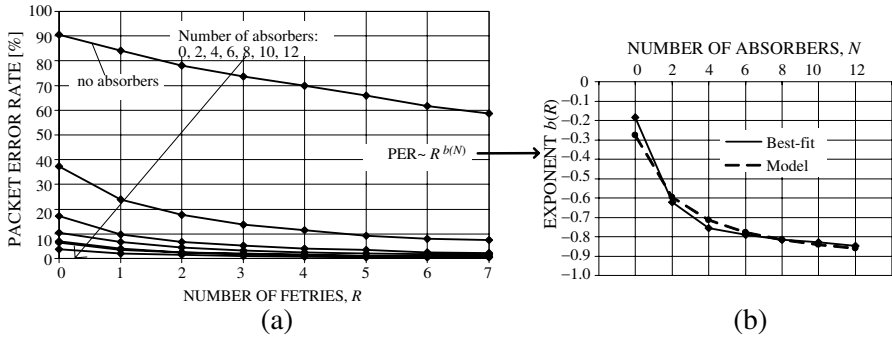| Number of retries	0	1	2	3	4	5	6	7
Exponent 'b'	-1.222	-1.289	-1.334	-1.373	-1.412	-1.465	-1.451	-1.523

Figure 6. Measurements of PER as (a) a function of the number of retries; (b) a plot of $b(N)$ exponent.

the more abruptly the curve tends to a "safe" PER level close to or below 1% PER$_{thr}$) which is usually regarded as a threshold PER for an acceptable transmission quality.

$$b(R) = -0.0399 \cdot R - 1.2042 \tag{13}$$

8. PER AS A FUNCTION OF THE NUMBER OF TRANSMISSION REPETITIONS

The last investigated topic was concerned with evaluating the impact of the number of allowed retries R on ZigBee resilience in the presence of multipath signal components. Again the reverberation chamber load was varied from zero up to 12 absorbers. As shown in Fig. 6(a) ZigBee appears to be very sensitive to heavy multipath (in the absence of absorbers), showing a dramatic improvement by 53.2% in PER between zero and two absorbers. Quite expectedly, further loading resulted in successive diminishing of PER although the advantages were less conspicuous than in the initial case. The decline was exponential in all curves, given by a general form PER $\sim R^{b(N)}$. Interestingly, even in the most overloaded case (i.e., 12 absorbers) PER was still above the acceptable PER$_{thr} = 1\%$ if no repetitions were admitted. PER$_{thr}$ threshold was intersected for the first time with 6 absorbers

(which corresponds to $\tau_{\text{rms}} = 0.37\,\mu s$) and 6 retries. With 12 absorbers (which corresponds to $\tau_{\text{rms}} = 0.20\,\mu s$) PER_{thr} was obtained with only 3 retries. Another observation regarding PER vs. R is that the gradient of descent of PER with R proved to be growing with successive loading of the chamber in such a manner that the more load was placed in the resonant cavity the faster the PER curve was diminishing for a given R. It is best presented in Fig. 6(b) where the exponent $b(N)$ of this exponential growth is drawn together with best-fit model matched to it and defined by Equation (14).

Of course, the improvement associated with the use of retries does not come at no price. The major penalty related to the use of multiple retries consists in the linear increase of the total transmission delay D_{tot} with increasing R, which can be problematic in some applications. As was determined by means of measurements, each packet retransmission introduces extra delay τ_R equal to 9.5 ms into D_{tot}. Moreover, one should recall from Section 3 that one of the characteristic features of ZigBee — one that makes it an eligible solution for mesh sensor networks (see chpt. 5.3 in [20]) — is its inherent ability to deliver packets by multiple hops via intermediate nodes. Each of these hops, in turn, causes additional delay τ_h of 8.1 ms. It is therefore easy to calculate that if there is a message to be transferred via a chain of M devices (thus making $M-1$ hops) and assuming that each packet will be retransmitted R times, an extra transmission delay D_{ex} by which D_{tot} will be increased, is given by Equation (15). The radiowave propagation delay has been omitted in this formula due to short operational ranges of ZigBee devices (on the order of a few hundred meters at most).

$$b(N) = 0.724 \cdot N^{-0.847} \qquad (14)$$
$$D_{ex} = \tau_R \cdot R \cdot [\tau_h \cdot (M-1)] \qquad (15)$$

9. CONCLUSIONS

The paper presents results of intensive research related to the ZigBee system performance in environments representing different multipath conditions. Such a scalable variety of multipath conditions have been achieved in a reverberation chamber by means of its controlled loading (investigated in-depth by the authors in one of their previous publications) with absorbers. With the knowledge of the radio channel time response in the chamber with different amount of load, three items were investigated regarding ZigBee operation. Firstly, it was determined that the multipath effect had a highly non-uniform effect on different ZigBee channels for a lightly loaded chamber. While

more absorbers were placed inside, this impact became increasingly uniform over all 16 channels available in the 2.4 ISM band. Secondly, an exponential profile of the Packet Error Rate was confirmed vs. the number of absorbers and related to a particular propagation environment type. It was thus proved that ZigBee can be expected to work well under multipath conditions present in indoors and open spaces, to which ZigBee is in fact most dedicated. Thirdly, an exponential improvement in PER was demonstrated with a stepwise increase in the number of retries. Repetitions were thus shown — in quality and quantity — to be an effective and commendable means for effectively combating negative multipath effects. However, the number of retries itself should be carefully adjusted in order to avoid excessive retransmissions leading to unnecessary transmission delays harmful to time-sensitive applications.

ACKNOWLEDGMENT

REFERENCES

1. Alejos, A. V., M. Garcia Sánchez, I. Cuinas, and J. C. G. Valladares, "Sensor area network for active RTLS in RFID tracking applications at 2.4 GHz," *Progress In Electromagnetics Research*, Vol. 110, 43–58, 2010.

2. Mitilineos, S. A., D. M. Kyriazanos, O. E. Segou, J. N. Goufas, and S. C. A. Thomopoulos, "Indoor localisation with wireless sensor networks," *Progress In Electromagnetics Research*, Vol. 109, 441–474, 2010.

3. Jamlos, M. F. B., A. R. B. Tharek, M. R. B. Kamarudin, P. Saad, M. A. Shamsudin, and A. M. M. Dahlan, "A novel adaptive Wi-Fi system with RFID technology," *Progress In Electromagnetics Research*, Vol. 108, 417–432, 2010.

4. Gross, N., "21 ideas for the 21st century," *Business Week*, 78–167, Aug. 30, 1999.

5. Alsehaili, M., S. Noghanian, A. R. Sebak, and D. A. Buchanan,

"Angle and time of arrival statistics of a three dimensional geometrical scattering channel model for indoor and outdoor propagation environments," *Progress In Electromagnetics Research*, Vol. 109, 191–209, 2010.

6. Ndzi, D. L., K. Stuart, S. Toautachone, B. Vuksanovic, and D. Sanders, "Wideband sounder for dynamic and static wireless channel characterisation: Urban picocell channel model," *Progress In Electromagnetics Research*, Vol. 113, 285–312, 2011.

7. ITU, "Propagation data for the terrestrial land mobile service in the vhf and uhf bands," ITU-R P.1145, 1995.

8. ITU, "Multipath propagation and parameterization of its characteristics," ITU-R P.1407, 2003.

9. Rappaport, T. S., *Wireless Communications. Principles and Practice*, 2nd Edition, Prentice Hall, 2002.

10. Cuiñas, I. and M. G. Sánchez, "Measuring, modelling, and characterizing of indoor radio channel at 5.8 GHz," *IEEE Transactions on Vehicular Technology*, Vol. 50, No. 2, 526–535, Mar. 2001.

11. Wysocki, T. A. and H. J. Zepernick, "Characterization of the indoor radio propagation channel at 2.4 GHz," *Journal of Telecommunications and Information Technology*, 3–4, 2001.

12. Dillard, C. L., "A study of rough surface scattering phenomena in the LMDS band (28 GHz)," Master's Thesis, Blacksburg, Virginia, Feb. 27, 2003.

13. Janssen, G. J. M., P. A. Stigter, and R. Prasad, "Wideband indoor channel measurements and BER analysis of frequency selective multipath channels at 2.4, 4.75 and 11.5 GHz," *IEEE Transactions on Communications*, Vol. 44, No. 10, 1272–1288, Oct. 1996.

14. Moraitis, N., A. Kanatas, G. Pantos, and P. Constantinou, "Delay spread measurements and characterization in a special propagation environment for PCS microcells," *Proc. IEEE 13th International Symposium on Personal, Indoor and Mobile Radio Communications*, Vol. 3, 1190–1194, Sep. 2002.

15. Fleury, B. H., "An uncertainty relation for WSS processes and its application to WSSUS systems," *IEEE Transactions on Communications*, Vol. 44, No. 12, 1632–1634, Dec. 1996.

16. Hashemi, H., "The indoor radio propagation channel," *IEEE Proceedings*, Vol. 81, No. 7, 943–968, Jul. 1993.

17. Andersen, J. B., "Radio channel characterisation," COST 231 Final Report, COST Office, European Commission, Brussels, Belgium, 1999.

18. Saunders, S. R., *Antennas and Propagation for Wireless Communication Systems*, 2nd Edition, John Wiley & Sons, 2007.

19. Chuang, J. C., "The effects of time delay spread on portable radio communications channels with digital modulation," *IEEE Journal on Selected Areas in Communications*, Vol. 5, No. 5, 879–889, Jun. 1987.

20. IEEE, "IEEE Std 802.15.4-2006, Part 15.4: Wireless medium access control (MAC) and physical layer (PHY) specification for low-rate wireless personal area networks (WPANs)," 1–320, 2006.

21. Centeno, A. and N. Alford, "Measurement of zigbee wireless communications in mode-stirred and mode-tuned reverberation chamber," *Progress In Electromagnetics Research M*, Vol. 18, 171–178, 2011.

22. Hope, D., J. Dawson, A. Marvin, M. Panitz, C. Christopoulos, and P. Sewell, "Assessing the performance of ZigBee in a reverberant environment using a mode stirred chamber," *Proc. IEEE International Symposium on Electromagnetic Compatibility — EMC Europe 2008*, 1–6, Hamburg, Sep. 18–22, 2008, doi: 10.1109/ISEMC.2008.4652116.

23. Genender, E., C. L. Holloway, K. A. Remley, J. Ladbury, G. Koepke, and H. Garbe, "Use of reverberation chamber to simulate the power delay profile of a wireless environment," *Proc. International Symposium on Electromagnetic Compatibility — EMC Europe 2008*, 1–6, Hamburg, Sep. 8–12, 2008, doi: 10.1109/EMCEUROPE.2008.4786832.

24. Orlenius, C., M. Franzen, P. S. Kildal, and U. Carlberg, "Investigation of heavily loaded reverberation chamber for testing of wideband wireless units," *Proc. IEEE Society International Symposium on Antennas and Propagation*, 3569–3572, Albuquerque, NM, USA, Jul. 9–14, 2006.

25. Pomianek, A. J., K. Staniec, and Z. Jóskiewicz, "Practical remarks on measurement and simulation methods to emulate the wireless channel in the reverberation chamber," *Progress In Electromagnetics Research*, Vol. 105, 49–69, 2010.

26. Mariani Primiani, V. and F. Moglie, "Numerical simulation of LOS and NLOS conditions for an antenna inside a reverberation chamber," *Journal of Electromagnetic Waves and Applications*, Vol. 24, Nos. 17–18, 2319–2331, 2010.

27. Staniec, K. and A. J. Pomianek, "On simulating the radio signal propagation in the reverberation chamber with the ray launching method," *Progress In Electromagnetics Research B*, Vol. 27, 83–99, 2011.

28. Reza, A. W., M. S. Sarker, and K. Dimyati, "A novel integrated mathematical approach of ray-tracing and genetic algorithm for optimizing indoor wireless coverage," *Progress In Electromagnetics Research*, Vol. 110, 147–162, 2010.

29. Gao, P. C., Y. B. Tao, and H. Lin, "Fast RCS prediction using multiresolution shooting and bouncing ray method on the GPU," *Progress In Electromagnetics Research*, Vol. 107, 187–202, 2010

30. Sarker, M. S., A. W. Reza, and K. Dimyati, "A novel ray-tracing technique for indoor radio signal prediction," *Journal of Electromagnetic Waves and Applications*, Vol. 25, Nos. 8–9, 1179–1190, 2011.